Journal of Alloys and Compounds 505 (2010) 243–248

Contents lists available at ScienceDirect

Journal of Alloys and Compounds

journal homepage: www.elsevier.com/locate/jallcom

Preparation and photocatalytic activity of TiO_2 nanotube powders derived by a rapid anodization process

Yulong Liao, Wenxiu Que*

Electronic Materials Research Laboratory, School of Electronic and Information Engineering, Xi'an Jiaotong University, Xi'an 710049, Shaanxi, PR China

ARTICLE INFO

Article history:
Received 28 April 2010
Received in revised form 5 June 2010
Accepted 10 June 2010
Available online 18 June 2010

Keywords:
TiO_2 nanotube
Rapid anodization
Methyl orange
Photocatalytic degradation

ABSTRACT

TiO_2 nanotube powders as a photocatalyst for water processing were prepared by a rapid anodization process in a perchlorate containing electrolyte. Morphological and micro-structural properties of the TiO_2 nanotube powders were carefully characterized. Results indicate that the TiO_2 nanotubes with high aspect ratio, perfect tubular architecture, and smooth surface were successfully synthesized by a one-step electrochemical process. It is also noted that the nanotubes grow rather rapidly and well ordered in bundles with about 3 μm in length, 15 nm in outer diameter, and 10 nm in inner diameter. Effects of synthesis temperature of water bath on the morphological properties of the TiO_2 nanotubes were also studied, and a crystalline transformation process from amorphous to anatase then to rutile was revealed as the annealing temperature rises. Methyl orange was taken as a model compound to confirm the photocatalytic activities of the as-synthesized TiO_2 nanotube powders with different crystal structures. It is found that when annealed at 550 °C, the TiO_2 nanotube powders with a mixing phase structure of anatase and rutile have the best photocatalytic degradation activity for the methyl orange aqueous solution.

1. Introduction

During the past decades, environmental problems such as water and air pollution have attracted worldwide attentions, and many fundamental and applied researches on environmental remediation have been carried out [1–3]. In particular, photocatalysts on the base of TiO_2 show a promising and potential application for water treatment, due to high catalytic activity, low cost, good mechanical and chemical stability, and non-toxicity to human beings and environment [4–6]. It has been reported that the nanotubular TiO_2 owns a better photochemical reactivity than bulk TiO_2 particles [7–9]. Moreover, A large specific surface area of the nanotubular TiO_2 also results in the enhancement of its photocatalytic activity [10]. Therefore, the nanotubular TiO_2 has been intensively studied and various methods have been adopted to prepare TiO_2 nanotubes or nanotube arrays in recent years, including anodic oxidation [11,12], hydrothermal treatment [13,14], and template synthesis [15,16], etc.

Among these fabrication routes, the anodization of titanium (Ti) is an attractive way for synthesizing a highly ordered nanotube arrays in recent years. During the anodization processing, TiO_2 nanotube arrays are gradually formed on the surface of Ti sheet or Ti film deposited conductive glass mainly in a fluoride containing electrolyte, and their photocatalytic activities are also been investigated. However, to our best of knowledge, up to now there have few reports on the preparation of the TiO_2 nanotube (NT)-powders in the perchlorate containing electrolyte, and the photocatalytic activity of the TiO_2 NT-powders derived by the rapid anodization process has not yet been reported in detail so far. Although Ref. [17] reported that the rapid anodization process was used to synthesize the titania nanotube powders in aqueous electrolytes of NaCl and $HClO_4$, they discussed mainly the properties of the titania nanotube powders synthesized in the NaCl electrolyte, and the titania nanotube powders obtained from the $HClO_4$ containing electrolyte is only for a comparison. That is to say, the preparation process and the photocatalytic properties of the TiO_2 NT-powders derived by the rapid anodization process in perchlorate containing electrolyte have not been studied and reported in detail.

As we know, heat treatment temperature has a tight relationship with the crystalline form of the TiO_2 NT-powders, and the crystalline form of the TiO_2 has great impact on its photocatalytic activity. The anatase phase is believed to have a better photocatalytic activity than the others including rutile and brookite phases, but there are still disagreements of the effects of the TiO_2 crystalline structure on its photocatalytic activity [18–20]. Therefore, it is necessary to further study the effects of the heat treatment temperature on the photocatalytic activities of the TiO_2 NT-powders.

Here, we report what we believe to be the first study on the photocatalytic activities of the TiO_2 NT-powders derived by the rapid anodization processing in the perchlorate containing electrolyte.

---

* Corresponding author. Tel.: +86 29 82668679; fax: +86 29 82668794.
E-mail address: wxque@mail.xjtu.edu.cn (W. Que).

0925-8388/$ – see front matter © 2010 Elsevier B.V. All rights reserved.
doi:10.1016/j.jallcom.2010.06.038

Firstly, the preparation processing was presented and discussed in detail. Then a chemical mechanism was presented to explain the formation of the TiO_2 NT-powders during the preparation. Morphological and micro-structural properties of the as-prepared TiO_2 NT-powders were characterized and discussed. Effects of the heat treatment temperature on the crystalline properties of the TiO_2 NT-powders were also carefully studied, followed by a discussion of the photocatalytic activities of the TiO_2 NT-powder photocatalysts derived with different heat treatment temperatures.

2. Experimental

2.1. Materials

Titanium foils (99.5% purity, 0.2 mm in thick) were purchased from General Research Institute for Nonferrous Metals, China. Before the rapid anodization process, they were carefully washed by foamless eradicator, cleaned by sonicating in acetone and ethanol, and then rinsed with deionized (DI) water and dried in oven at 60 °C. $HClO_4$ and methyl orange are analytical pure and were purchased from Sinopharm Group Chemical Reagent Co. Ltd., China.

2.2. Preparation of TiO_2 NT-powder photocatalysts

The TiO_2 NT-powders were synthesized by the rapid anodization process of titanium (Ti) foil from the perchlorate ions containing electrolyte. A large piece of raw Ti foil was cut into small pieces with the same regular shape (4 cm × 4 cm), followed by a cleaning process as mentioned before. One piece of the as-cleaned Ti sheet was taken as the working electrode and a platinum (Pt) foil as the counter electrode, and then they were directly immersed into the electrolyte, which is an aqueous solution of 0.15 M $HClO_4$. A DC power supply (Model GPS-3303c, GW Instrument Co., Ltd., Taiwan) was employed to provide a constant potential of 20 V across the two electrodes with a distance of 2.5 cm. Thus, the rapid anodization process was conducted in a two-electrode reaction chamber, in which the Ti foil was used as the anode and a Pt foil of the same size as the cathode. The schematic of the anodization process was shown as Fig. 1. The reaction chamber was then put in a water bath with different reaction temperatures. It should be mentioned that magnetic stirring was being carried out throughout the anodization process. Afterward, the solution containing TiO_2 precipitation was filtered, washed with DI water and centrifuged several times. The derived powders were oven dried at 70 °C for 8 h and thus the white TiO_2 NT-powders were obtained. The reaction temperature of the water bath was set at 5 °C, 25 °C, and 55 °C, respectively, during the rapid anodization process. Correspondingly, the samples were named as Powder-5 °C, Powder-25 °C and Powder-55 °C. Powder-25 °C was further annealed at different temperatures of 300 °C, 450 °C, 550 °C, and 700 °C for 3 h with a heating rate of 5 °C/min at an electric muffle furnace.

2.3. Characterization

Field emission scanning electron microscopy (FESEM, JSM-7000F, JEOL Inc., Japan) and transmission electron microscopy (TEM, JEM2100, JEOL Inc., Japan) were used to characterize the morphological and structural properties of the TiO_2 NT-powders. The TEM was operated under an acceleration voltage of 200 kV. FESEM observation was carried out with an acceleration voltage of 20 kV. The micro-structural properties of the TiO_2 NT-powders were characterized by a X-ray diffraction (XRD) analyzer using a D/max-2400 X-ray diffraction spectrometer (Rigaku) with Cu Kα radiation and operated at 40 kV and 100 mA from 20° to 70°, and the scanning speed was $15^\circ\ min^{-1}$ at a step of 0.02°. The analyte concentrations of the methyl orange (MO) were measured by the UV–vis absorption spectrum from JASCO V-570 UV/VIS/NIR spectrometer in a range of wavelength from 300 nm to 650 nm.

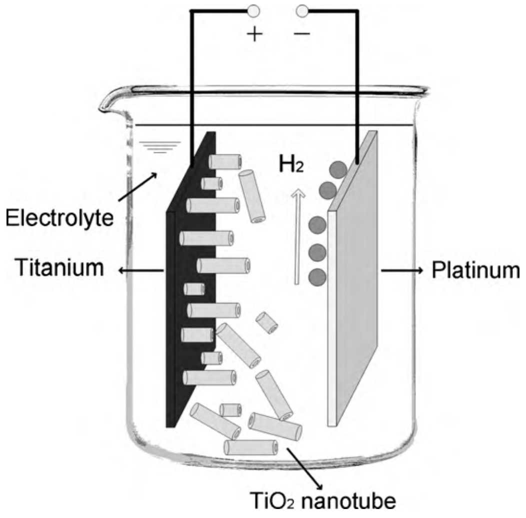

Fig. 1. Schematic diagram of the anodization processing.

2.4. Photocatalytic activity measurements

Methyl orange (MO), which is a kind of the azo dye known to be carcinogenic and mutagenic, was usually selected as a model dye to evaluate the photocatalytic performance of the different photocatalysts [21,22]. In this paper, the MO was thus selected as the model dye with a concentration of 0.02 g/L. To evaluate the photocatalytic activity of the TiO_2 NT-powders with different crystalline structures, a series of tests were carried out as follows: The TiO_2 NT-powders photocatalysts of 0.3 g/L were added into the MO solution, dispersed by a sonicating for 5 min, and stirred by a magnetic bar for another 2 h to reach the adsorption/desorption equilibrium. Then the suspension solution put in quartz reactor was illuminated by an UV light with a 300 W high pressure mercury lamp. Magnetic stirring was being carried out during the photocatalytic testing. The whole system including the mercury lamp and reactant suspension solution was maintained at room temperature by a flow of cooling water. Certain volume of the dye suspension solutions was withdrawn at a sequence of time intervals. After centrifugation, the residue MO was measured by the UV–vis spectrophotometer, and thus the percentage of the MO degradation can be obtained.

3. Results and discussion

With the DC power supply starting to work, vigorous gas bubbles are immediately generated at the cathode, while the color of the Ti foil (as the anode) is turned into purple at the surface. A few minutes later, white precipitations start to produce from the Ti foil and then diffuse into the electrolyte until the whole Ti foil is totally oxidized into white precipitations. Thus, about 3 g TiO_2 NT-powders can be obtained within 50 min. It should be mentioned here that the anodization processing is accomplished in 50 min, which indicates that the TiO_2 NT-powders is rapidly prepared with a growth rate of 5×10^3 nm/min. This anodization processing is schematically shown in Fig. 1.

Formation mechanism of the TiO_2 NT-powders can be explained as follows: at the cathode, hydrogen is generated throughout the experiment until Ti foil is totally dissolved into the electrolyte, and the hydrogen generation occurres via the following reaction

$$4H^+ + 4e^- \rightarrow 2H_2 \uparrow \text{(cathode)} \tag{1}$$

At the anode, the Ti sheet is originally oxidized and formed a thin TiO_2 layer at the surface via the following reaction

$$Ti + 2H_2O \rightarrow 4H^+ + 4e^- + TiO_2 \downarrow \text{(anode)} \tag{2}$$

The TiO_2 thin layer is responsible for the purple surface of the Ti foil observed at the beginning stage of the experiment. Then the TiO_2 thin layer begins to dissolve and transform into TiO_2 NT-powders with the help of a strong electric field produced by the DC power supply and the perchlorate containing electrolyte.

Samples of the TiO_2 NT-powders prepared at different temperatures are characterized by FESEM as shown in Fig. 2. Results indicate that the TiO_2 NT-powders can be easily obtained by the rapid anodization process under different temperatures of water bath. It can be observed from Fig. 2(b) that the nanotubes are highly ordered and stacked in bundles and are from 0.5 μm to several μm in length and very small in diameter, indicating that the as-prepared nanotubes own a high aspect ratio (more than 10^2). Actually, the FESEM image of the sample Powder-25 °C shows clearer nanotubular morphology and more obvious structure as compared with those of the samples Powder-5 °C and Powder-55 °C as shown in Fig. 2(a) and (c), respectively. In addition to, it is also very convenient for the preparation of the TiO_2 nanotubes at room temperature (25 °C). Therefore, the sample Powder-25 °C is further studied in the following sections.

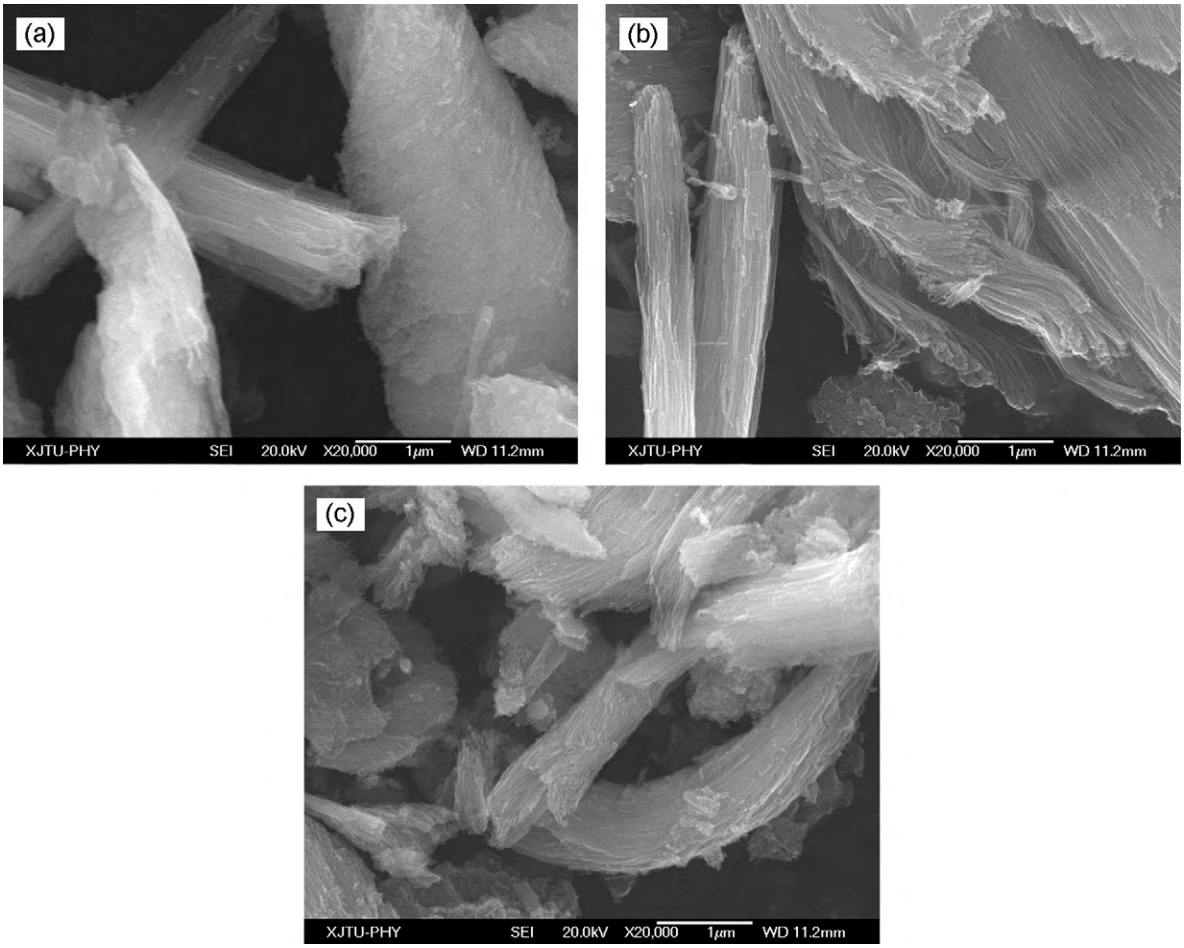

Fig. 2. FESEM images of the as-prepared TiO_2 NT-powders synthesized at different temperatures. (a) 5 °C, (b) 25 °C, and (c) 55 °C.

A further confirmation of the nanostructural properties of the TiO_2 NT-powders was observed by TEM and Fig. 3 shows the TEM images, indicating that the TiO_2 powders with nanotube structure can be obtained at 25 °C. It is also noted that the nanotubes grow rather rapidly and have a highly ordered in bundles with about 3 μm in length and 15 nm in diameter, which corresponds to an aspect ratio of 2×10^2. Fig. 3(a) shows that the outer and the inner diameters of the nanotubes are about 15 nm and 10 nm, respectively. It should be mentioned here that it is possible to change the diameter a little by changing synthetic protocols, but the changing range is very limited. These similar results were also reported in Ref. [23], which the geometry of the individual tubes were not evidently affected by changes in the conditions such as electrolyte concentration (from 0.01 M to 3 M) and applied potential (15 V, 20 V and 60 V). Results also indicate that the as-prepared NT-powers are composed of uniform nanotube structure without other architecture, and these nanotubes are stacked close to each other in the form of the NT-bundle as shown in Fig. 3(b). Some fingerprint patterns can be also observed from Fig. 3(c), it is probably related to the slight crystallization of the TiO_2 nanotubes. The downside inset of Fig. 3(c) shows the selected area electron diffraction (SAED) pattern of the nanotubes. Obviously, a composite pattern of the diffuse rings and several broad diffuse rings can be seen, which indicates that the as-prepared TiO_2 NT-powders show an amorphous structure with little crystallization. The upper inset of Fig. 3(c) shows the XRD pattern of the sample Powder-25 °C. It can be seen from the XRD pattern that several diffraction peaks can be found and they can be assigned to specific lattice planes of the anatase phase of TiO_2 (JCPDS Patterns No. 21-1272). These XRD results indicate that the as-prepared TiO_2 NT-powders mainly still stay in amorphous, but with a little crystallization in anatase, which is good in line with the results revealed by TEM.

It can be concluded based on above results that highly ordered and well structured TiO_2 NT-powders with high respect ratio can be synthesized by the rapid anodization process in 0.15 M $HClO_4$ aqueous electrolyte. The as-synthesized TiO_2 NT-powders without annealing are incompletely crystallized and most of them are still in amorphous. Therefore, the as-synthesized TiO_2 NT-powders should put into further heat treatment so as to improve the crystalline properties.

Fig. 4 shows the FESEM images of the sample Powder-25 °C annealed at 300 °C, 550 °C, and 700 °C, respectively. It should be mentioned that the heat treatment should be carefully carried out at a low heating rate of 5 °C/min, so as to avoid a damage or collapse of the nanotubular structure of the TiO_2 NT-powders due to a heating. It can be seen from Fig. 4(a) and (b) that the nanotubular structure of these samples can be maintained well and the heat treatment below 550 °C does not destroy the morphological properties of the nanotubes. However, with increase the heat treatment temperature up to 700 °C, some crystal grains as shown in Fig. 4(c) can be clearly observed and the size of these crystal grains becomes rather big (more than 200 nm in diameter). These results indicate that the initial nanotubular configuration of the sample is probably destroyed due to a higher heat treatment temperature. It should be stressed that the nanotubular configuration of the TiO_2 NT-powders can be maintained well below a heat treatment temperature of 550 °C, it is very important for the as-prepared TiO_2 NT-powders to have a high aspect ratio and a good photo-

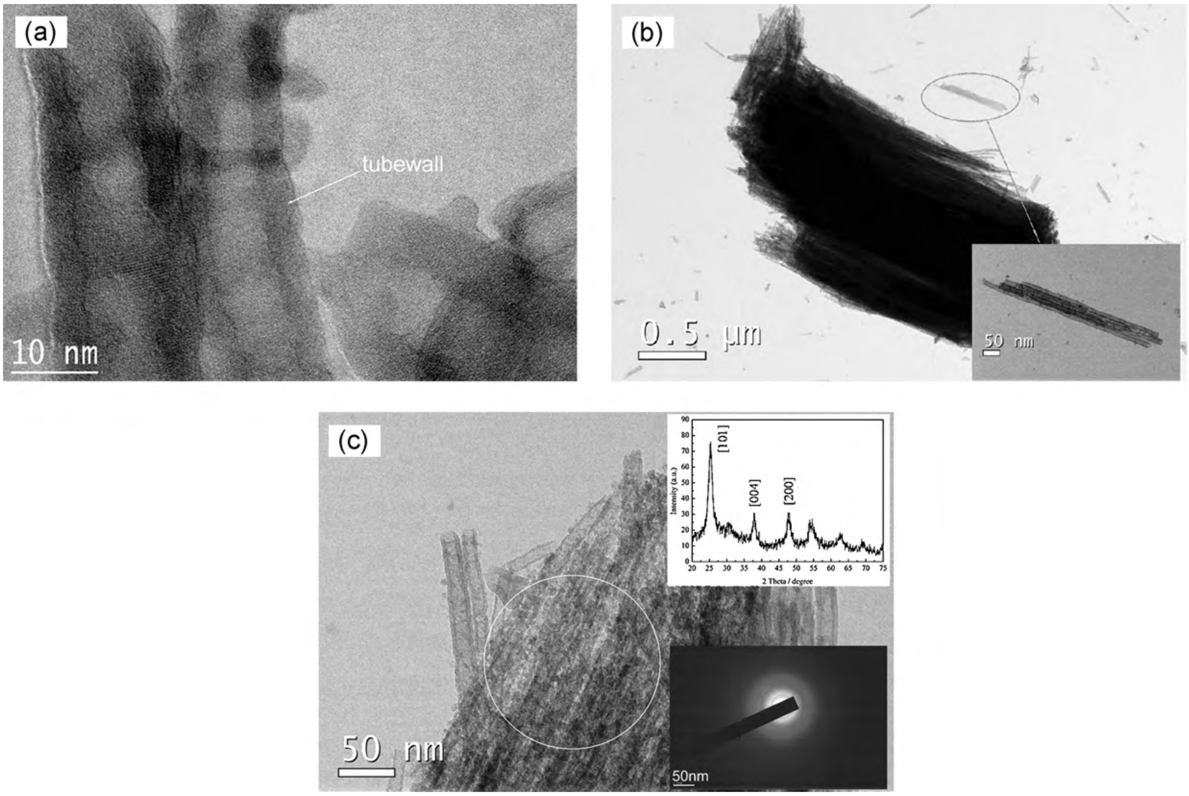

Fig. 3. TEM images of the sample Powder-25 °C.

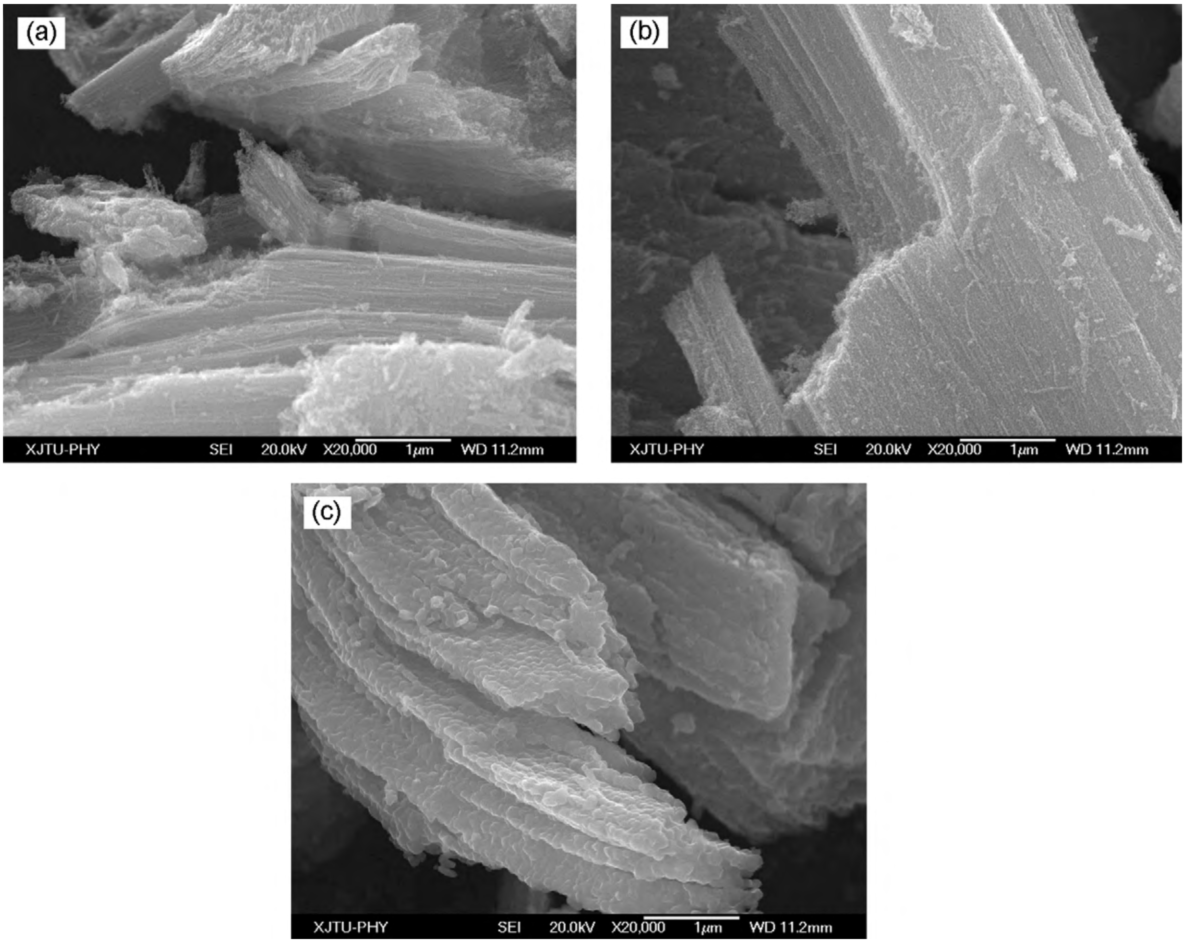

Fig. 4. FESEM images of the sample Powder-25 °C annealed at (a) 300 °C, (b) 550 °C, and (c) 700 °C.

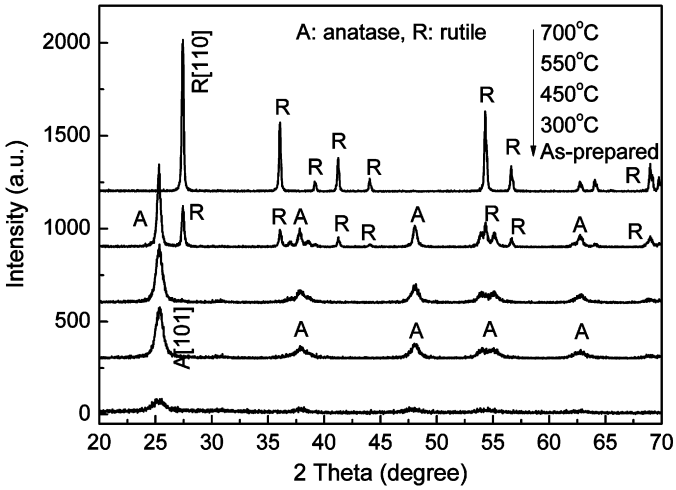

Fig. 5. XRD patterns of the TiO_2 NT-powders annealed at different temperatures.

catalytic property. Our results are basically agreement with those as reported in Refs. [17,24], but Ref. [17] reported that the TiO_2 nanotube can be stable up to 600 °C and Ref. [24] reported that the collapsing of the nanotube structure occurs when annealed at 880 °C and the nanotubular configuration can be maintained over 570 °C. These differences should be related to the different preparation process of the samples.

Fig. 5 shows the XRD patterns of the sample Powder-25 °C annealed at different temperatures. It can be seen that the sample Powder-25 °C only has a very weak diffraction signal as compared to the annealed samples, which indicates only slight crystallization of the as-synthesized TiO_2 NT-powders if there is no further annealing process. However, strong diffraction peaks can be clearly seen for all the annealed samples, indicating that the annealed samples are well crystallized after the heat treatment from 300 °C to 700 °C. The results also indicate that there are only anatase diffraction peaks to have been observed for the samples annealed at 300 °C and 450 °C, which means that the TiO_2 NT-powders are well crystallized only in anatase phase below a heat treatment of 450 °C. But as the heat treatment temperature increases to 550 °C, a clear signal of the rutile diffraction peaks starts to appear, indicating that the sample contains both anatase and rutile phase when annealed at 550 °C. With further increase the heat treatment temperature up to 700 °C, only rutile diffraction peaks are observed, the diffraction peak at [1 1 0] in intensity is very strong and the full width at half maximum (FWHM) of this main peak is quite small, these indicate that the TiO_2 NT-powders are well crystallized with large crystal grains. In addition to, the mean crystalline size (noted as d_a) of the anatase TiO_2 NT-powders annealed at different temperatures are calculated from the Scherrer equation [25], and the results are summarized in Table 1. It can be noted from Table 1 that a crystalline transformation of the TiO_2 NT-powders from amorphous to rutile can be clearly observed with increase the heat treatment temperature to 700 °C. It can be also found that the FWHM of the main peaks (anatase [1 0 1] and rutile [1 1 0]) decreases as the heat treatment temperature rises from 300 °C to 450 °C, and the size of the corresponding crystal grains increases from 7.622 nm to 16.37 nm, which is probably due to the increase of the heating temperatures offering a higher energy for the growth of the crystal grains. When the heating temperature increases to 550 °C, the Scherrer equation is no more available to calculate the d_a value. However, it can be estimated from the FESEM image as shown in Fig. 4(c) that the d_a is over 200 nm when the TiO_2 NT-powders annealed at 700 °C. Obviously, these results concluded from Table 1 provide a further confirmation of those results obtained by TEM and FESEM.

Table 1
Crystal structure properties of the TiO_2 NT-powders.

Synthesis conditions	Crystalline form	FWHM	d_a (nm)
As-prepared	Amorphous	1.123	7.622
Annealed at 300 °C	Anatase	0.616	13.895
Annealed at 450 °C	Anatase	0.526	16.373
Annealed at 550 °C	Anatase + rutile	0.379	
Annealed at 700 °C	Rutile		

TiO_2 are well known as photocatalyst for the photodecomposition of organic compounds, the oxidation reaction can be described as follows

$$\text{organic} + O_2 \xrightarrow{TiO_2} CO_2 + H_2O + m\ \text{acides} \qquad (3)$$

where m acids (mineral acids) are originally from hetero atoms, such as S, N and Cl, in the organic components. The absorption values (Abs) of the MO solution as a function of the light wavelength at different periods are shown in Fig. 6. At first, the MO solution without addition of the TiO_2 NT-powders was irradiated by the UV only, and the corresponding UV-spectra at different irradiation periods in a range of the light wavelength from 300 nm to 650 nm are shown in Fig. 6(a). It can be seen that the MO is only slight photo-degraded under UV irradiation of 100 min. Fig. 6(b) shows the photocatalytic degradation of the MO with an addition of the TiO_2 NT-powders annealed at 550 °C, and the Abs value of the MO solution decrease almost to zero in 80 min, which indicates that the addition of the

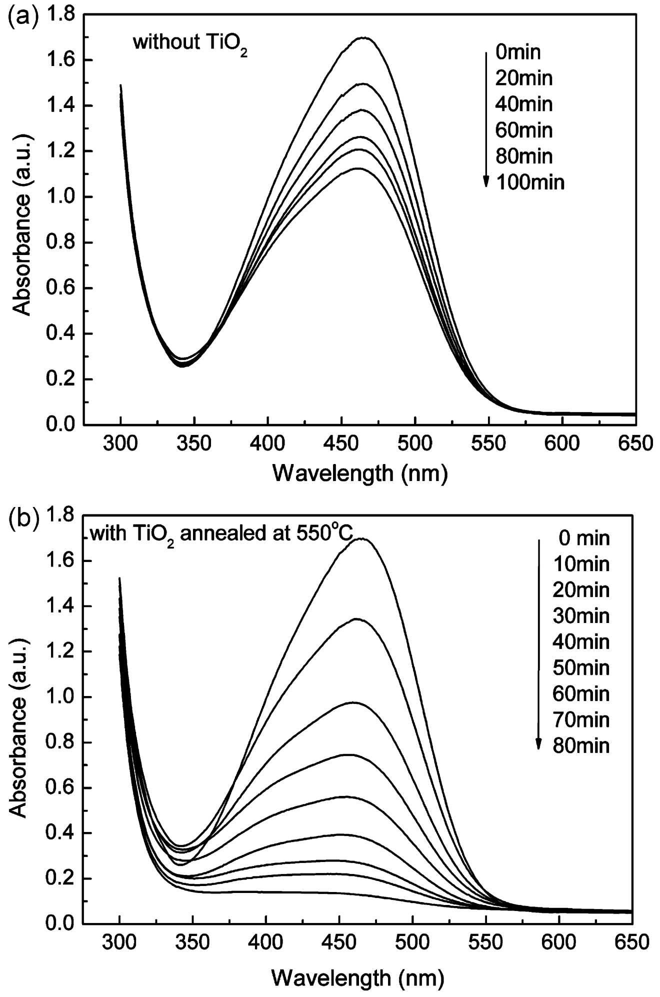

Fig. 6. UV–vis spectra of the MO solution degraded without (a) and with (b) the TiO_2 NT-powders.

TiO_2 NT-powders can obviously accelerate the degradation of the MO under UV irradiation.

The TiO_2 NT-powders annealed at 300 °C, 450 °C, 550 °C, and 700 °C are also used to estimate their photocatalytic activities, respectively, and similar results are observed. Furthermore, a comparison of their photocatalytic activities is necessary. It can be seen from Fig. 6 that the main absorption peak of the MO solution appears at about 463 nm, which corresponds to the maximum absorbance value of the MO aqueous solution. Based on the Beer–Lambert law [26]

$$Abs = \varepsilon bc \tag{4}$$

where Abs is the measured absorbance, ε is the wavelength-dependent molar absorptivity coefficient, b is the path length, and c is the analyte concentration, thus $c/c_0 = A/A_0$ can be easily obtained, where c_0 is the initial concentration of the MO, A_0 is the absorbance value at 463 nm of the MO aqueous solution before UV irradiation. Consequently, based on $c/c_0 = A/A_0$, comparison of the photocatalytic activities of the TiO_2 NT-powders annealed at different temperatures is shown in Fig. 7. It can be revealed from Fig. 7 as follows: (a) irradiated by UV light for 100 min for the pure MO solution, only 30% of the 20 ppm MO is photo-degraded, indicating that the MO aqueous solution is stable enough as the module compound for the investigation of the photocatalytic activities of the TiO_2 NT-powders; (b) for the TiO_2 NT-powders annealed at 300 °C, 450 °C, and 550 °C, the MO can be sharply photocatalytically degraded under UV photo-irradiation within 80 min; (c) the photocatalytic activities increase as the heat treatment temperature rises from 300 °C to 550 °C. One possible explanation for this phenomenon is that the increase of the photocatalytic activities of the TiO_2 NT-powders result from the better crystallization and the coexistence of the rutile and anatase phase, which might play a key role on the charge transfer and the separation of electron–hole pairs as the increase of the heat treatment temperature [11]; (d) the TiO_2 NT-powders annealed at 700 °C nearly has no photocatalytic activity for the degradation of the MO aqueous solution, this indicates that the rutile TiO_2 has poor photocatalytic properties. Another possible explanation is that when the TiO_2 NT-powders is annealed at 700 °C, overage growth of the crystal grains with more than 200 nm in diameter leads to a collapsing of the nanotubular configuration, which sharply reduces the activity areas, and thereby results in the poor photocatalytic activity. Based on the above results and discussion, it can be concluded that the optimum post-heat treatment temperature is at 550 °C, which the TiO_2 NT-powders own the best photocatalytic activity due to a coexistence of anatase and rutile crystal structures. It should be mentioned here that the as-synthesized TiO_2 NT-powders over Ti sheets have not shown as efficient photocatalytic activity as the commercial Degussa P-25 powders at present stage, but the photocatalytic activities of the TiO_2 NT-powders will be improved by optimizing various experimental conditions and further work is in progress.

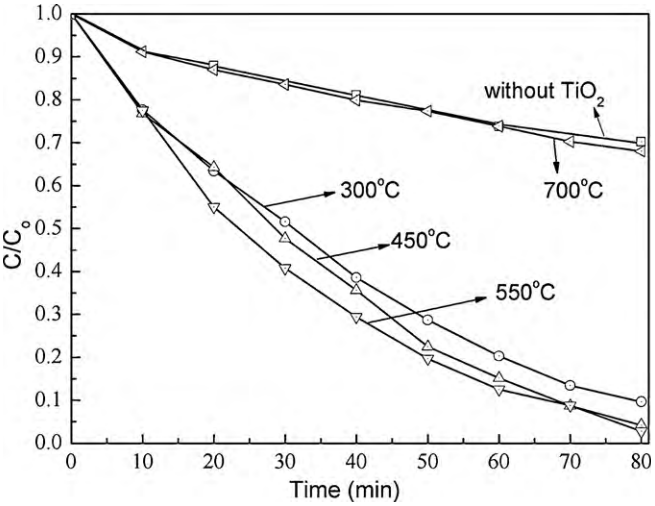

Fig. 7. Comparison of the photocatalytic activities of the TiO_2 NT-powders annealed at different temperatures.

4. Conclusions

The TiO_2 NT-powders have been prepared by the rapid anodization process in the 0.15 M $HClO_4$ aqueous electrolyte under a constant potential of 20 V. The as-prepared TiO_2 NT-powders have a perfect tubular configuration with smooth surface, which are well ordered in bundles with about 3 μm in length, 15 nm in outer diameter, and 10 nm in inner diameter. It has been also found that the synthesis temperature has an influence on the morphological properties of the TiO_2 nanotubes. With increase the post-heat treatment temperature from 300 °C to 700 °C, the crystal structure of the TiO_2 NT-powders transforms from pure anatase phase to pure rutile phase. All the NT-powders samples annealed below 700 °C have shown the photocatalytic ability for the MO degradation. Moreover, the TiO_2 NT-powders annealed at 550 °C, which has a coexistence of anatase and rutile crystal structures, have been proved to own the best photocatalytic activity. These results indicate that the rapid anodization process could be an interesting method to study the photocatalytic properties of the TiO_2 NT-powders.

Acknowledgments

This work was supported by the Major Program of the National Natural Science Foundation of China under Grant No. 90923012, the Ministry of Science and Technology of China through 863-project under grant 2009AA03Z218 and the Research Fund for the Doctoral Program of Higher Education of China under grant 200806980023.

References

[1] R. Ashid, T. Morikawa, T. Ohwaki, K. Aoki, Y. Taga, Science 293 (2001) 269–271.
[2] M. Fujihira, Y. Satoh, T. Osa, Nature 293 (1981) 206–208.
[3] M.R. Hoffmann, S.T. Martin, W. Choi, D.W. Bahnemann, Chem. Rev. 95 (1995) 69–96.
[4] C.C. Chen, C.S. Lu, Y.C. Chung, J.L. Jan, J. Hazard. Mater. 141 (2007) 520–528.
[5] A. Bravo, J. Garcia, X. Domenech, J. Peral, J. Chem. Res. (1993) 376–377.
[6] A.H. Pollema, E.B. Milosavljevic, J.L. Hendrix, L. Solujic, J.H. Nelson, Monatsh. Chem. 123 (1992) 333–339.
[7] J.M. Macak, M. Zlamal, J. Krysa, P. Schmuki, Small 3 (2007) 300–304.
[8] M.A. Khan, H.T. Jung, O.B. Yang, J. Phys. Chem. B 110 (2006) 6626–6630.
[9] Y.S. Chen, J.C. Crittenden, S. Hackney, L. Sutter, D.W. Hand, Environ. Sci. Technol. 39 (2005) 1201–1208.
[10] S. Pavasupreea, S. Ngamsinlapasathiana, Y. Suzukia, S. Yoshikawaa, Mater. Lett. 61 (2007) 2973–2977.
[11] H.C. Liang, X.Z. Li, J. Hazard. Mater. 162 (2009) 1415–1422.
[12] D.A. Wang, Y. Liu, B. Yu, F. Zhou, W.M. Liu, Chem. Mater. 21 (2009) 1198–1206.
[13] D.S. Seoa, J.K. Lee, H. Kimb, J. Cryst. Growth 229 (2001) 428–432.
[14] Y. Suzuki, S. Yoshikawa, J. Mater. Res. 19 (2004) 982–985.
[15] J.J. Qiu, W.D. Yu, X.D. Gao, X.M. Li, Nanotechnology 17 (2006) 4695–4698.
[16] J.H. Jung, H. Kobayashi, K.J.C. Bommel, S.J. Shinkai, T. Shimizu, Chem. Mater. 14 (2002) 1445–1447.
[17] N.F. Fahim, T. Sekino, Chem. Mater. 21 (2009) 1967–1979.
[18] H.Y. Zhu, X.P. Gao, Y. Lan, D.Y. Song, Y.X. Xi, J.C. Zhao, J. Am. Chem. Soc. 126 (2004) 8380–8381.
[19] J.G. Yu, H.G. Yu, B. Cheng, C. Trapalis, J. Mol. Catal. A: Chem. 249 (2006) 135–142.
[20] N. Masahashi, Y. Mizukoshia, S. Semboshib, N. Ohtsu, Appl. Catal. B: Environ. 90 (2009) 255–261.
[21] H.M. Yang, K. Zhang, R.G. Shi, X.W. Li, X.D. Dong, Y.M. Yu, J. Alloys Compd. 413 (2006) 302–306.
[22] Y.S. Sohn, Y.R. Smith, M. Misra, V. Subramanian, Appl. Catal. B: Environ. 84 (2008) 372–378.
[23] R. Hahn, J.M. Macak, P. Schmuki, Electrochem. Commun. 9 (2007) 947–952.
[24] K. Varghese, D.W. Gong, M. Paulose, C.A. Grimes, E.C. Dickey, J. Mater. Res. 18 (2003) 156–165.
[25] H.P. Klug, L.E. Alexander, X-ray Diffraction Procedures for Polycrystalline and Amorphous Materials, John Wiley, New York/London, 1974.
[26] J.D.J. Ingle, S.R. Crouch, Spectrochemical Analysis, Prentice-Hall, New Jersey, 1988.